

$^{118}\text{Sn}(^{55}\text{Mn},3\text{n}\gamma)$ **2013Ha02**

Type	Author	History	Citation	Literature Cutoff Date
Full Evaluation	C. M. Baglin ¹ , E. A. Mccutchan ² , S. Basunia ¹		NDS 153, 1 (2018)	1-Oct-2018

E=260 MeV; stack of two 0.6 mg/cm² ^{118}Sn targets; Gammasphere detector array (101 Compton-suppressed Ge detectors); measured $E\gamma$, $I\gamma$, $\gamma\gamma$ coin, angular distribution ratios R.
Dataset includes $^{120}\text{Sn}(^{55}\text{Mn},5\text{n}\gamma)$, E=253 MeV.

 ^{170}Re Levels

E(level) [†]	J ^π [‡]	Comments
0.0		
0.0+x [@]	(9 ⁻)	Additional information 1.
0.0+y ^{&}	(10 ⁺)	Additional information 2.
83.20+x [#]	20 (10 ⁻)	
215.1+x [@]	3 (11 ⁻)	
263.80+y ^a	20 (11 ⁺)	
403.8+x [#]	3 (12 ⁻)	
543.3+y ^{&}	3 (12 ⁺)	
622.2+x [@]	3 (13 ⁻)	
817.4+y ^a	3 (13 ⁺)	
889.6+x [#]	3 (14 ⁻)	
1036.4+y ^{&}	3 (14 ⁺)	
1169.4+x [@]	3 (15 ⁻)	
1226.6+y ^a	3 (15 ⁺)	
1341.8+y ^{&}	4 (16 ⁺)	
1486.8+x [#]	4 (16 ⁻)	
1487.5+y ^a	4 (17 ⁺)	
1662.8+y ^{&}	5 (18 ⁺)	
1806.2+x [@]	4 (17 ⁻)	
1870.4+y ^a	5 (19 ⁺)	
2114.4+y ^{&}	5 (20 ⁺)	
2146.3+x [#]	4 (18 ⁻)	
2392.6+y ^a	5 (21 ⁺)	
2472.4+x [@]	4 (19 ⁻)	
2702.8+y ^{&}	5 (22 ⁺)	
2778.2+x [#]	4 (20 ⁻)	
3041.8+y ^a	5 (23 ⁺)	
3057.4+x [@]	4 (21 ⁻)	
3332.8+x [#]	4 (22 ⁻)	
3400.5+y ^{&}	6 (24 ⁺)	
3636.7+x [@]	4 (23 ⁻)	
3771.4+y ^a	6 (25 ⁺)	
3953.2+x [#]	4 (24 ⁻)	
4151.7+y ^{&}	6 (26 ⁺)	
4310.5+x [@]	5 (25 ⁻)	
4532.0+y ^a	6 (27 ⁺)	
4675.4+x [#]	5 (26 ⁻)	
4926.6+y ^{&}	6 (28 ⁺)	

Continued on next page (footnotes at end of table)

$^{118}\text{Sn}(\text{Mn},\text{3n}\gamma)$ 2013Ha02 (continued) ^{170}Re Levels (continued)

E(level) [†]	J [‡]	E(level) [†]	J [‡]	E(level) [†]	J [‡]	E(level) [†]	J [‡]
5084.9+x [@] 5	(27 ⁻)	5952.2+x [@] 5	(29 ⁻)	6899.2+x [@] 7	(31 ⁻)	7885.2+x [@] 9	(33 ⁻)
5322.1+y ^a 6	(29 ⁺)	6155.2+y ^a 7	(31 ⁺)	7049.2+y ^a 9	(33 ⁺)	7983.2+y ^a 10	(35 ⁺)
5494.7+x [#] 5	(28 ⁻)	6402.0+x [#] 5	(30 ⁻)	7371.0+x [#] 7	(32 ⁻)	8388.0+x [#] 9	(34 ⁻)
5736.3+y ^{&} 6	(30 ⁺)	6601.3+y ^{&} 8	(32 ⁺)	7517.3+y ^{&} 9	(34 ⁺)		

[†] From least squares fit to E γ , including lines with uncertain placement.[‡] Tentative values from 2013Ha02; see comments on bands. Consistent with deduced band structure and observed γ multipolarity.# Band(A): $\pi h_{11/2} \otimes v i_{13/2}$, $\alpha=0$. Tentative J $^\pi$ assigned by 2013Ha02 based on systematics of neighboring nuclei and configuration proposed for sequence. Initial alignment $\approx 6\hbar$; AB alignment blocked but BC alignment occurs At $\hbar\omega=0.29$ MeV, close to value predicted by cranked shell model, so $v i_{13/2}$ orbital is probably involved. The $\pi h_{11/2}$ orbital is yrast for low J In ^{169}Re . Observed B(M1)/B(E2) ratios agree well with those expected for the proposed configuration.[@] Band(a): $\pi h_{11/2} \otimes v i_{13/2}$, $\alpha=1$. See comment on signature partner band.[&] Band(B): $\pi h_{11/2} \otimes v h_{9/2}$, $\alpha=0$. Tentative J $^\pi$ assigned by 2013Ha02 based on proposed configuration (for which theoretical B(M1)/B(E2) ratios following the AB crossing agree with the experimental ones). An additional band crossing is observed At $\hbar\omega=0.37$ MeV, probably associated with a pair of $i_{13/2}$ quasineutrons.^a Band(b): $\pi h_{11/2} \otimes v h_{9/2}$, $\alpha=1$. See comment on signature partner band. $\gamma(^{170}\text{Re})$

E γ	I γ [†]	E $_l$ (level)	J $^{\pi}_i$	E $_f$	J $^{\pi}_f$	Mult. [‡]	Comments
x		0.0+x	(9 ⁻)	0.0			
83.2 2	$\approx 35^{\#}$	83.20+x	(10 ⁻)	0.0+x	(9 ⁻)		
115.2 2	8.0 6	1341.8+y	(16 ⁺)	1226.6+y	(15 ⁺)		
131.9 2	$\approx 95^{\#}$	215.1+x	(11 ⁻)	83.20+x	(10 ⁻)	D	Mult.: R=0.59 3.
145.7 2	19 2	1487.5+y	(17 ⁺)	1341.8+y	(16 ⁺)		
175.3 2	20 1	1662.8+y	(18 ⁺)	1487.5+y	(17 ⁺)		
188.6 2	$\approx 105^{\@}$	403.8+x	(12 ⁻)	215.1+x	(11 ⁻)	D	Mult.: R=0.59 2.
190.1 2	4.4 3	1226.6+y	(15 ⁺)	1036.4+y	(14 ⁺)		
207.6 2	19 2	1870.4+y	(19 ⁺)	1662.8+y	(18 ⁺)		
218.5 2	100 4	622.2+x	(13 ⁻)	403.8+x	(12 ⁻)	D	Mult.: R=0.62 2.
219.0 2	4.7 [@] 4	1036.4+y	(14 ⁺)	817.4+y	(13 ⁺)		
244.0 2	17 1	2114.4+y	(20 ⁺)	1870.4+y	(19 ⁺)		
263.8 2	$\approx 6^{\#}$	263.80+y	(11 ⁺)	0.0+y	(10 ⁺)		
267.4 2	90 5	889.6+x	(14 ⁻)	622.2+x	(13 ⁻)	D	Mult.: R=0.64 2.
274.1 2	2.9 2	817.4+y	(13 ⁺)	543.3+y	(12 ⁺)		
275.4 2	34 2	3332.8+x	(22 ⁻)	3057.4+x	(21 ⁻)	D	Mult.: R=0.57 2.
278.3 2	14 1	2392.6+y	(21 ⁺)	2114.4+y	(20 ⁺)		
279.1 2	37 4	3057.4+x	(21 ⁻)	2778.2+x	(20 ⁻)		Mult.: R=0.67 3 for doublet.
279.5 2	2.9 [#] 3	543.3+y	(12 ⁺)	263.80+y	(11 ⁺)		
279.7 2	76 8	1169.4+x	(15 ⁻)	889.6+x	(14 ⁻)		Mult.: R=0.67 3 for doublet.
303.8 2	30 3	3636.7+x	(23 ⁻)	3332.8+x	(22 ⁻)		Mult.: R=0.62 3 for doublet.
305.9 2	38 5	2778.2+x	(20 ⁻)	2472.4+x	(19 ⁻)		Mult.: R=0.62 3 for doublet.
310.2 2	16 1	2702.8+y	(22 ⁺)	2392.6+y	(21 ⁺)		
316.5 2	22 3	3953.2+x	(24 ⁻)	3636.7+x	(23 ⁻)		Mult.: R=0.65 3 for doublet.
317.4 2	67 4	1486.8+x	(16 ⁻)	1169.4+x	(15 ⁻)		Mult.: R=0.65 3 for doublet.
319.4 2	56 6	1806.2+x	(17 ⁻)	1486.8+x	(16 ⁻)		Mult.: R=0.65 3 for doublet.
320.6 2	$\approx 19^{\@}$	403.8+x	(12 ⁻)	83.20+x	(10 ⁻)		
326.1 2	43 3	2472.4+x	(19 ⁻)	2146.3+x	(18 ⁻)	D	Mult.: R=0.64 2.

Continued on next page (footnotes at end of table)

$^{118}\text{Sn}(^{55}\text{Mn},3\text{n}\gamma)$ **2013Ha02 (continued)** $\gamma(^{170}\text{Re})$ (continued)

E_γ	I_γ^\dagger	$E_i(\text{level})$	J_i^π	E_f	J_f^π	Mult. [‡]	Comments
339.0 2	17 1	3041.8+y	(23 ⁺)	2702.8+y	(22 ⁺)	D	Mult.: R=0.64 2.
340.1 2	45 3	2146.3+x	(18 ⁻)	1806.2+x	(17 ⁻)	D	Mult.: R=0.61 3.
357.3 2	19 1	4310.5+x	(25 ⁻)	3953.2+x	(24 ⁻)	D	Mult.: R=0.68 4.
358.6 2	12 1	3400.5+y	(24 ⁺)	3041.8+y	(23 ⁺)		
364.9 2	16 1	4675.4+x	(26 ⁻)	4310.5+x	(25 ⁻)	D	Mult.: R=0.68 4.
370.9 2	4.8 5	3771.4+y	(25 ⁺)	3400.5+y	(24 ⁺)		
380.3 2	7.6 8	4151.7+y	(26 ⁺)	3771.4+y	(25 ⁺)		
380.4 2	4.8 5	4532.0+y	(27 ⁺)	4151.7+y	(26 ⁺)		
394.6 2	3.8 4	4926.6+y	(28 ⁺)	4532.0+y	(27 ⁺)		
395.5 2	2.9 3	5322.1+y	(29 ⁺)	4926.6+y	(28 ⁺)		
407.1 2	$\approx 30^{\text{@}}$	622.2+x	(13 ⁻)	215.1+x	(11 ⁻)		
409.2 2	3.5 2	1226.6+y	(15 ⁺)	817.4+y	(13 ⁺)		
409.5 2	9.5 8	5084.9+x	(27 ⁻)	4675.4+x	(26 ⁻)		
409.8 2	7.1 6	5494.7+x	(28 ⁻)	5084.9+x	(27 ⁻)		
414.2 5	<2	5736.3+y	(30 ⁺)	5322.1+y	(29 ⁺)		
419.0 5	<2	6155.2+y	(31 ⁺)	5736.3+y	(30 ⁺)		
449.9 5	<2	6402.0+x	(30 ⁻)	5952.2+x	(29 ⁻)		
451.7 2	5.7 4	2114.4+y	(20 ⁺)	1662.8+y	(18 ⁺)		
457.5 2	4.4 2	5952.2+x	(29 ⁻)	5494.7+x	(28 ⁻)		
485.8 2	46 4	889.6+x	(14 ⁻)	403.8+x	(12 ⁻)		
493.1 2	3.5 $^{\text{@}}_3$	1036.4+y	(14 ⁺)	543.3+y	(12 ⁺)		
522.2 2	8.7 6	2392.6+y	(21 ⁺)	1870.4+y	(19 ⁺)		
547.2 2	49 4	1169.4+x	(15 ⁻)	622.2+x	(13 ⁻)	Q	Mult.: R=0.99 8.
553.6 2	4.7 3	817.4+y	(13 ⁺)	263.80+y	(11 ⁺)		Mult.: R=0.78 6; low for $\Delta J=2$ transition implied by level scheme.
554.6 2	23 2	3332.8+x	(22 ⁻)	2778.2+x	(20 ⁻)		Mult.: R=1.02 8.
579.3 2	14 1	3636.7+x	(23 ⁻)	3057.4+x	(21 ⁻)	Q	Mult.: R=0.72 3; low for $\Delta J=2$ transition implied by level scheme.
585.0 2	36 3	3057.4+x	(21 ⁻)	2472.4+x	(19 ⁻)		Mult.: R=1.03 8.
588.4 2	9.8 7	2702.8+y	(22 ⁺)	2114.4+y	(20 ⁺)		Mult.: R=1.05 5.
597.2 2	47 3	1486.8+x	(16 ⁻)	889.6+x	(14 ⁻)		Mult.: R=0.98 4.
620.4 2	20 2	3953.2+x	(24 ⁻)	3332.8+x	(22 ⁻)	Q	Mult.: R=0.94 4.
631.9 2	27 2	2778.2+x	(20 ⁻)	2146.3+x	(18 ⁻)	Q	Mult.: R=0.99 8.
636.9 2	52 3	1806.2+x	(17 ⁻)	1169.4+x	(15 ⁻)	Q	Mult.: R=0.98 8.
649.2 2	15 1	3041.8+y	(23 ⁺)	2392.6+y	(21 ⁺)		
659.5 2	40 3	2146.3+x	(18 ⁻)	1486.8+x	(16 ⁻)	Q	
666.1 2	42 3	2472.4+x	(19 ⁻)	1806.2+x	(17 ⁻)	Q	
673.9 2	10.0 7	4310.5+x	(25 ⁻)	3636.7+x	(23 ⁻)		
697.6 2	9.9 7	3400.5+y	(24 ⁺)	2702.8+y	(22 ⁺)		
722.2 2	10 1	4675.4+x	(26 ⁻)	3953.2+x	(24 ⁻)		
729.6 2	7.2 5	3771.4+y	(25 ⁺)	3041.8+y	(23 ⁺)		
751.3 2	7.8 6	4151.7+y	(26 ⁺)	3400.5+y	(24 ⁺)		
760.6 2	7.6 5	4532.0+y	(27 ⁺)	3771.4+y	(25 ⁺)		
774.4 2	7.9 5	5084.9+x	(27 ⁻)	4310.5+x	(25 ⁻)		
774.8 2	6.1 4	4926.6+y	(28 ⁺)	4151.7+y	(26 ⁺)		
790.1 2	3.8 3	5322.1+y	(29 ⁺)	4532.0+y	(27 ⁺)		
809.7 2	2.9 2	5736.3+y	(30 ⁺)	4926.6+y	(28 ⁺)		
819.3 2	8.0 6	5494.7+x	(28 ⁻)	4675.4+x	(26 ⁻)		
833.0 5	<2	6155.2+y	(31 ⁺)	5322.1+y	(29 ⁺)		
865.0 5	<2	6601.3+y	(32 ⁺)	5736.3+y	(30 ⁺)		
867.3 2	5.0 3	5952.2+x	(29 ⁻)	5084.9+x	(27 ⁻)		
894.0 5	<2	7049.2+y	(33 ⁺)	6155.2+y	(31 ⁺)		
907.3 2	2.9 3	6402.0+x	(30 ⁻)	5494.7+x	(28 ⁻)		
916.0 $^{\text{@}}_5$	<2	7517.3+y?	(34 ⁺)	6601.3+y	(32 ⁺)		
934.0 $^{\text{@}}_5$	<2	7983.2+y?	(35 ⁺)	7049.2+y	(33 ⁺)		

Continued on next page (footnotes at end of table)

$^{118}\text{Sn}(^{55}\text{Mn},3\text{n}\gamma)$ 2013Ha02 (continued) $\gamma(^{170}\text{Re})$ (continued)

E_γ	I_γ^\dagger	$E_i(\text{level})$	J_i^π	E_f	J_f^π
947.0	5	<2	6899.2+x	(31 ⁻)	5952.2+x (29 ⁻)
969.0	5	<2	7371.0+x	(32 ⁻)	6402.0+x (30 ⁻)
986.0	5	<2	7885.2+x	(33 ⁻)	6899.2+x (31 ⁻)
1017.0	5	<2	8388.0+x	(34 ⁻)	7371.0+x (32 ⁻)

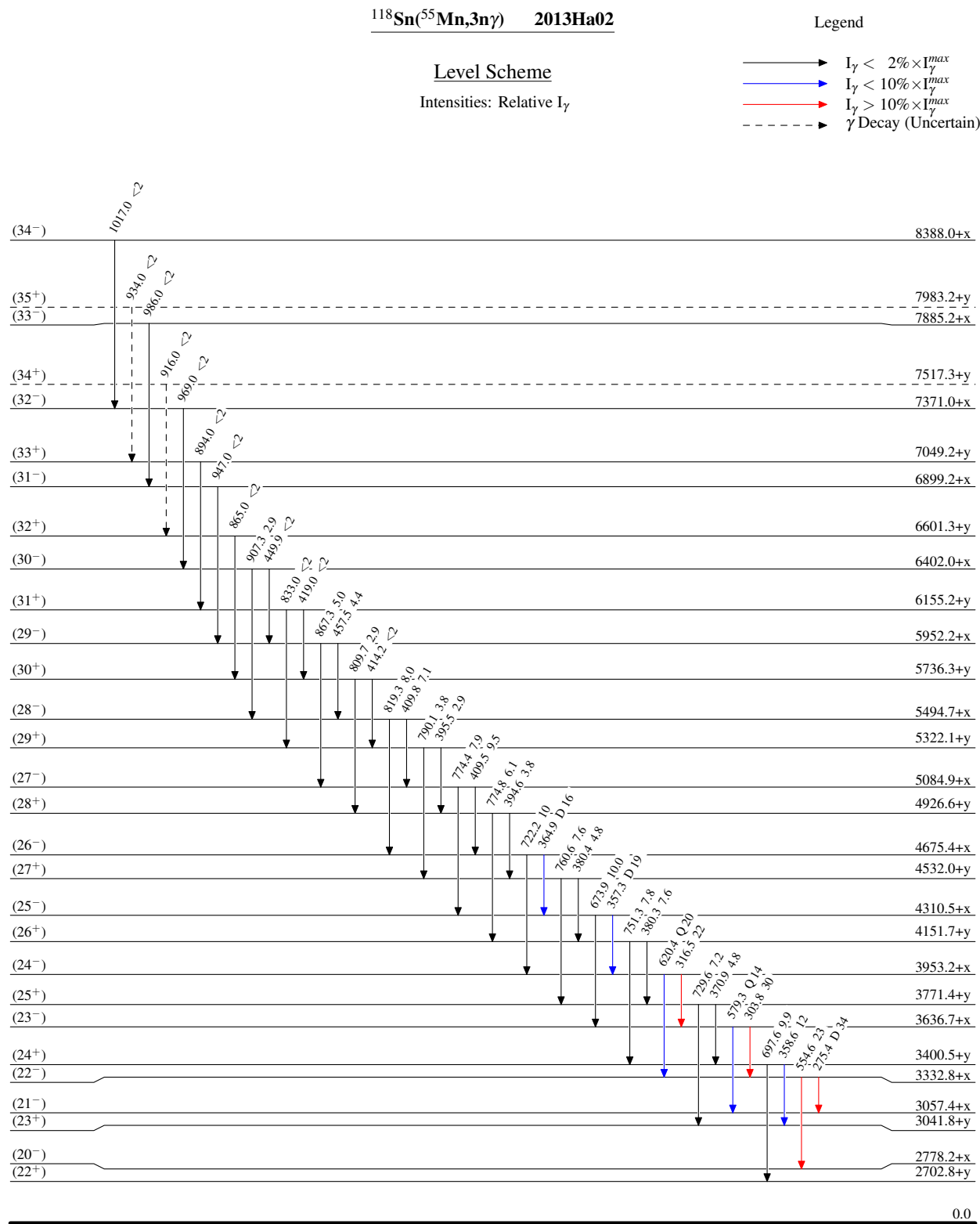
[†] Intensity relative to $I(219\gamma)=100$.

[‡] Assigned by evaluator based on R, the ratio of summed I_y from the 5 rings of detectors nearest to 90° (71°, 81°, 90°, 99°, 101°) to that from detectors At backward angles (122°, 130°, 143°, 148°, 163°), normalized so known pure D ($\Delta J=1$) and pure Q ($\Delta J=2$) transitions have values of R=0.6 and 1.0, respectively.

[#] Estimated by authors based on intensity balance.

[@] Estimated by authors based on intensity balance and branching ratio.

[&] Placement of transition in the level scheme is uncertain.



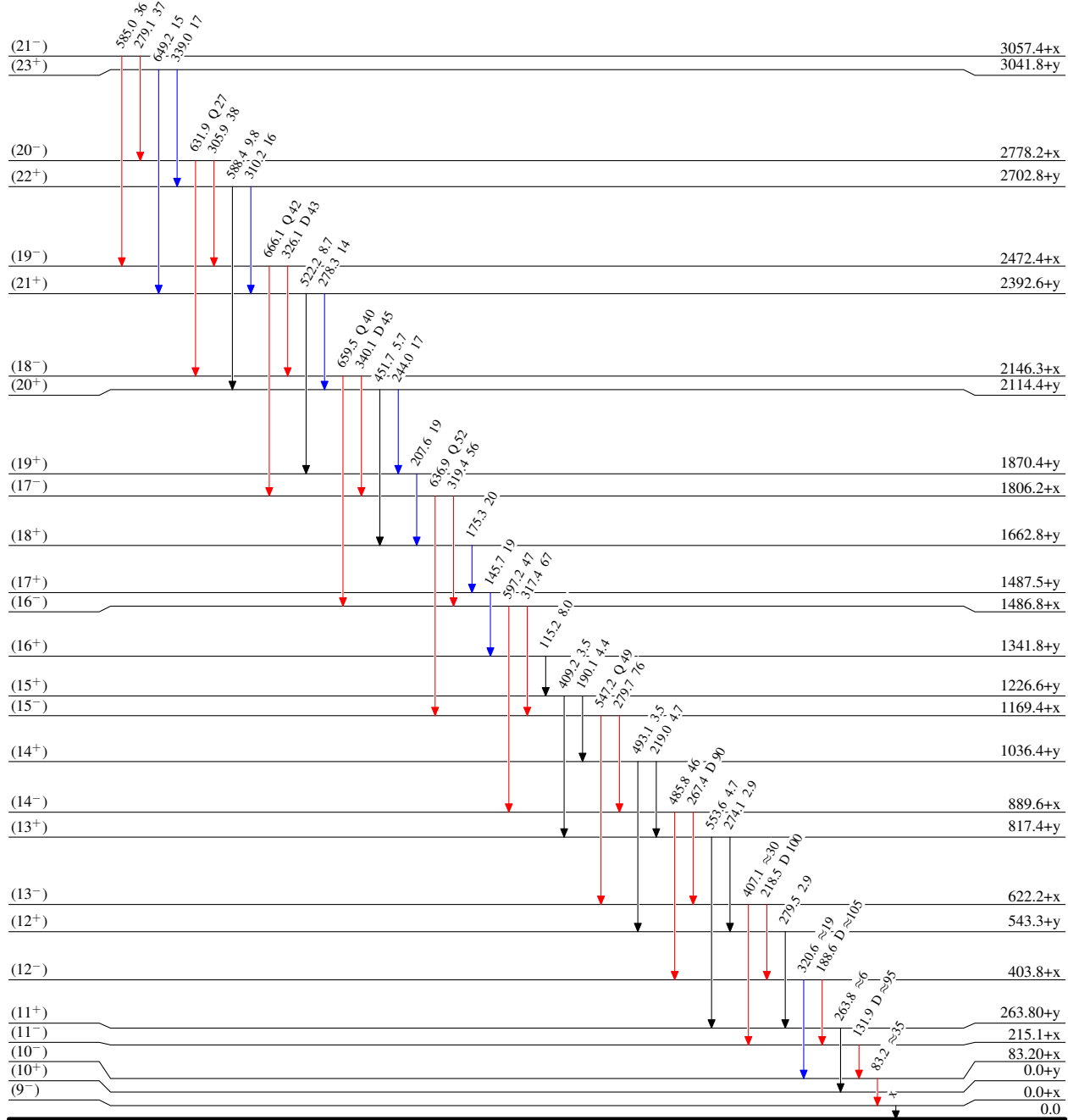
$^{118}\text{Sn}(\text{Mn},3\text{n}\gamma)$ 2013Ha02

Level Scheme (continued)

Intensities: Relative I_γ

Legend

- \longrightarrow $I_\gamma < 2\% \times I_\gamma^{\max}$
- $\xrightarrow{\quad}$ $I_\gamma < 10\% \times I_\gamma^{\max}$
- $\xrightarrow{\quad}$ $I_\gamma > 10\% \times I_\gamma^{\max}$



$^{118}\text{Sn}(\text{Mn},3\text{n}\gamma)$ 2013Ha02

Band(A): $\pi h_{11/2} \otimes vi_{13/2}$,
 $\alpha=0$

(34⁻) 8388.0+x

1017

(32⁻) 7371.0+x

969

(30⁻) 6402.0+x

907

(28⁻) 5494.7+x

819

(26⁻) 4675.4+x

722

(24⁻) 3953.2+x

620

(22⁻) 3332.8+x

555

(20⁻) 2778.2+x

632

(18⁻) 2146.3+x

660

(16⁻) 1486.8+x

597

(14⁻) 889.6+x

486

(12⁻) 403.8+x(10⁻) 321**Band(a):** $\pi h_{11/2} \otimes vi_{13/2}$, $\alpha=1$ (33⁻) 7885.2+x

986

(31⁻) 6899.2+x

947

(29⁻) 5952.2+x

867

(27⁻) 5084.9+x

774

(25⁻) 4310.5+x

674

(23⁻) 3636.7+x

579

(21⁻) 3057.4+x

585

(19⁻) 2472.4+x

666

(17⁻) 1806.2+x

637

(15⁻) 1169.4+x

547

(13⁻) 622.2+x

407

(11⁻) 215.1+x

0.0+x

Band(b): $\pi h_{11/2} \otimes vh_{9/2}$, $\alpha=1$ (35⁺) 7983.2+y

934

(34⁺) 7517.3+y

916

(32⁺) 6601.3+y

865

(30⁺) 5736.3+y

810

(28⁺) 4926.6+y

775

(26⁺) 4151.7+y

751

(24⁺) 3400.5+y

698

(22⁺) 2702.8+y

588

(20⁺) 2114.4+y

452

(18⁺) 1662.8+y

493

(16⁺) 1341.8+y

543.3+y

(14⁺) 1036.4+y(12⁺) 493(10⁺) 0.0+y